UNIVERSITY OF CALIFORNIA,
IRVINE

Integration of microfluidic chip with Loop-mediated Isothermal Amplification (LAMP) assay for rapid quantification of *Enterococcus Faecalis*

THESIS

submitted in partial satisfaction of the requirements
for the degree of

MASTER OF SCIENCE

in Engineering

by

Muyue Han

Dissertation Committee:
Professor Sunny Jiang, Ph.D, Chair
Professor Abraham Lee, PhD
Professor Diego Rosso, PhD

2018

TABLE OF CONTENTS

LIST OF FIGURES

Page

LIST OF TABLES

ACKNOWLEDGMENTS

I would like to thank all the people who have contributed to the work described in this thesis. This thesis would not have been possible without your support and encouragement.

First and foremost, I would like to express my gratitude and appreciation to my academic supervisor, Professor Sunny Jiang for the inspirational advice and guidance that she has given me over the past two years.

I would like to express my great appreciation to my committee members Professor Abraham Lee and Professor Diego Rosso for their support and guidance in improving this thesis manuscript.

I would like to thank Dr. Gopakumar Kamalakshakurup, Dr. Eric (Xiao) Huang, Dr Xingyu Lin, and Hamsa Gowda for providing useful feedback and suggestions during my experiments. Thanks to all the members in Applied & Environmental Microbiology lab and Biomolecular Microsystems and Nano Transducers (BioMiNT) lab.

I am grateful for the financial support from Bill and Melinda Gates Foundation (Grant Number OPP1111252), National Institutes of Health (NIH) under Prime Award no. UL1 TR001414, and The Regents of the University of California.

Finally, I would like to acknowledge my family for their constant love and support. I am fortunate to have met Lingxiang Yun at UC, Irvine. Thank you for supporting me, and I love you.

ABSTRACT OF THE THESIS

Integration of microfluidic chip with Loop-mediated Isothermal Amplification (LAMP) assay for rapid quantification of *Enterococcus Faecalis*

By

Muyue Han

Master of science in Engineering

University of California, Irvine, 2018

Professor Sunny Jiang, Ph.D, Chair

Rapid and sensitive monitoring of water quality can effectively prevent accidental human exposure to waterborne pathogens. In this project, a rapid quantification method was developed for *Enterococcusfaecalis*, a fecal indicator bacterium (FIB), used as a surrogate for water quality assurance. The loop-mediated isothermal amplification (LAMP) assay was combined with a microfluidic technology to produce thousands of individual reactions that convert the qualitative LAMP assay to quantitative results based on Poisson distribution. This "Lab on a Chip" (LOC) assay is considerably more rapid than the conventional culture-based and the polymerase chain reaction (PCR) based methods (i.e. qPCR and droplet digital PCR). The isothermal amplification removes the need of thermal cycling, which makes it suitable for field development. In this assay, the water sample is mixed with LAMP reagents in the presence of fluorescent dye. The mixture is then dispersed into thousands of droplets encapsulated within the oil phase using a microfluidic droplet generator chip, where each droplet acts as an individual LAMP reaction. By counting the number of positive droplets among total droplets in the viewing field, the most probable number of the *E.faecalis* can be quantified statistically. Several types and compositions of oil phases were tested for the compatibility with sample/LAMP reagent mixture for droplet generation and stability. The optimized oil phase can generate monodisperse droplets of 55 μm in diameter,

which were stable during LAMP reaction at 65°C for 30 mins. The droplets that stained with dsDNA fluorescent dye could be clearly visualized using fluorescence microscope and counted by image J software. The limit of detection of droplet LAMP assay is 4 $cfu/reaction$ in pure culture.

Chapter 1

Introduction

The global burden of waterborne disease owing to unsafe drinking water, inadequate or non-existent sanitation and hygiene is a major challenge to public health and can be associated with significant financial burden. The challenges of unsafe water quality are not limited to developing countries. In the U.S., 90 recreational water-associated outbreaks were reported by public health officials from 32 states and Puerto Rico, which resulted in at least 1788 cases and 95 hospitalizations during 2011-2012(https://www.cdc.gov/healthywater/surveillance/drinking-surveillance-reports.html). In addition, natural or manmade disasters may also deteriorate the local environment and trigger locally waterborne-disease outbreaks. For example, massive power outage as a common side effect of devastating disasters may cause wastewater treatment plant malfunction, which may lead to the discharge of untreated or inadequately treated sewage water to the environment. The disease-causing pathogens carried by human sewage may further spread and contaminate local aqueous environment and drinking water sources. Moreover, in hurricane-induced disasters, flood invasion can couple with power failure and contributes to widespread sanitary sewer overflows, which may increase the chances of waterborne infection and exacerbate the health problem throughout the local communities. Therefore, a field-applicable microbial pathogen

diagnostic system is critically needed for reducing or eliminating the accidental exposure to waterborne pathogens, especially in resource-limit regions and post-disaster situations. However, the deployment of current pathogen detection technologies is limited by the requirement of dedicated laboratory facilities with clean water, power and well-trained personnel, which prevents the timely collection of data and estimation of the local microbial contamination level and evaluation of waterborne-disease outbreak severity.

In this project, a microfluidic chip based droplet LAMP method was developed for the simultaneous detection and quantification of microbial pathogens. *Enterococcus Faecalis*, a fecal indicator bacterium, was used as a model microorganism for method demonstration. The goal is to develop a rapid, sensitive, economical pathogen quantification kit that is easy to perform in the field by personal with minimal training.

Chapter 2

Literature Review

2.1 Waterborne disease

Pathogenic microorganisms (i.e., viruses, bacteria, and protozoan parasites) may enter the water system through point sources (e.g. the discharge of municipal sewage and industrial effluents) and non-point sources (e.g. the runoff from residential and agricultural areas, and sewer overflow) (Girones et al. 2010). Contaminated water serves as a carrier of the infectious agents and transmits waterborne diseases such as dysentery, cholera, typhoid fever. People may come into contact with the infectious agents through contaminated drinking water, washing, and bathing or recreational water. Among 1415 recognized species of pathogenic microorganisms, approximately 25 per cent can cause infectious water-related infectious diseases (Yang et al. 2012). Waterborne disease as a worldwide burden had and continues to have a significant socioeconomic impact on human society. It is estimated that waterborne diseases due to the exposure to microbial pathogens are responsible for 2.2 million deaths every year, with an estimated economic loss of nearly 12 billion US dollars per year (Ramírez-Castillo et al. 2015). Children are most susceptible to waterborne diseases, in par-

ticular, diarrhea is responsible for 9 % of under five year old mortality worldwide (Carvajal-Vélez et al. 2016). According to the WHO/UNICEF Joint Monitoring Programme report (WHO/UNICEF 2015), 32 % of the global population still lack improved sanitation facility. Even in developed regions, several waterborne outbreaks were reported; During 2009-2010, 33 outbreaks associated with drinking water were reported in the United States by 17 states, involving 1,040 cases of illness, and 9 deaths. (Hilborn et al. 2013). In general, implementation of sanitation programs can be contributive to the improvement of safety of drinking water; meanwhile, the universal access to adequate sanitation and hygiene is instrumental in mitigating the morbidity and mortality caused by contaminated water in the long run. Additionally, effective methods for categorization and quantification of pathogenic microorganisms are also indispensable to water quality monitoring and microbial risk assessment. Furthermore, a reliable water quality monitoring system is also required to prevent the accidental human exposure to pathogens effectively and to control the mortality caused by contaminated water.

2.2 Waterborne microbial pathogens

Raw sewage water harbors a wide variety of pathogenic microorganisms that can initiate waterborne infections. The water-transmissivity of pathogens depends on several factors, for instance, pathogen's survival and replication in aquatic environments, the infective dose required to infect and cause diseases in the host, which is also associated with the pathogenicity of microorganisms (i.e. the virulence and the ability for multiplication) and host susceptibility (e.g. children, seniors and immunosuppressed patients may be more susceptible to infections). Consequently, it is crucial to differentiate different types of pathogens. The three major categories of pathogenic agents are bacterial pathogens, viral pathogens, and protozoan parasites. The common waterborne infectious agents are listed in table 2.1.

Pathogen	Associated disease
Bacteria:	
E. coli O157:H7	Diarrhea, hemolytic uremic syndrome (HUS)
Legionella pneumophila	Respiratory illness, legionellosis
Salmonella Typhi	Typhoid fever
Shigella spp.	Shigellosis
Vibrio cholerae	Gastroenteritis, cholera
Campylobacter jejuni	Gastroenteritis
Yersinia enterocolitica	Gastroenteritis
Pseudomonas aeruginosa	Infection can involve Respiratory tract, urinary tract, and gastrointestinal tract.
Virus:	
Adenovirus	Gastroenteritis, respiratory disease
Astrovirus	Gastroenteritis
Enterovirus	Paralysis, meningitis, skin rush
Hepatitis A virus	Hepatitis
Hepatitis E virus	Acute hepatitis
Norovirus	Gastroenteritis
Rotavirus	Gastroenteritis
Sapovirus	Gastroenteritis
Protozoa:	
Acanthamoeba spp.	Amoebic meningoencephalitis, keratitis
Cryptosporidium parvum	Cryptosporidiosis
Giardia lamblia	Diarrhea
Toxoplasma gondii	Toxoplasmosis, miscarriage

Table 2.1: A summary of waterborne pathogens and associated diseases

2.3 Pathogen indicators

Considering the complexity and diversity of microbial pathogens that excreted through feces and transmitted in environmental water bodies, the microbiological examination of all types of pathogenic microorganisms is cost-intensive and time-consuming, thereby, microbial indicator organisms have been recommended and used for evaluating sanitary quality of water with respect to the existence of fecal contamination, the treatment efficiency in drinking water and wastewater treatment plants, and the measurement of water quality for water reuse associated purposes. Ideally, the microbial indicator should meet a set of criteria to ensure the consistency and credibility of the measurement of microbial water quality, for instance, the indicators should consistently present in the feces, be almost equally resistant to environmental fluctuations and disinfection processes as pathogenic organisms, unable to proliferate in environment, and indicate a significant correlation among elevated level of indicators, the presence of enteric pathogen and the rate of gastrointestinal illness.

A group of organisms has been adopted as pathogen indicator as they are ubiquitous in the gastrointestinal tracts of human and warm-blooded animals and therefore the presence of these indicators may possibly signal fecal contamination and potential pathogen dissemination. Fecal indicator bacteria (FIB) including total coliforms, fecal coliforms, Escherichia coli, and enterococci ($E.faecalis$ and $E.faecium$) have been used as surrogates in the determination of microbiological impairment of water, identification and assessment of potential adverse health effect derived from undesired exposure to microbial hazards. These bacterial indicators are routinely tested in developed regions because of its simple and low cost detection and enumeration procedures (EPA 2012; Lin and Ganesh 2013; Bonjoch et al. 2004). Despite the convenience and simplicity of water microbial quality monitoring provided by FIB, it should be emphasized that numerous limitations also associate with their uses in investigating the source and extent of fecal pollution. Several studies have reported the failure cases in using aforementioned FIB species as fecal contamination markers, for example,

their short survival due to sunlight inactivation(Sinton et al. 2002), naturally existence in vegetation and soil (Ferguson and Signoretto 2011), comparatively high environmental persistence, the potential adaptation to non-host environments and possible naturalization in temperate sediments, subtropical and tropical aquatic environments(Anderson et al. 2005; Rochelle-Newall et al. 2015). In consequence, these commonly used FIB species are unable to satisfy the criteria for ideal indicators of fecal contamination, and therefore are insufficient to identify the origins of fecal contamination and assess the magnitude of contamination.

To circumvent the problem of persistence and regrowth of conventional FIB in environment, some alternative microbial and chemical indicators have been proposed to be used in conjunction with traditional FIB measurement to mitigate the false positive results and provide a better prediction of occurrence of pathogens and potential health risks. For instance, fecal anaerobes (*Bacteroides spp.* and *Bifidobacterium spp.*) have received great attention as promising candidate indicators for recent or extensive fecal contamination due to their short survival in aerobic environment; moreover, some strains of *Bacteroids* and *Bifidobacterium* species have high host-specificity, which is contrary to the ubiquity of coliforms, thereby being proposed as prospective markers for distinguishing between human-originated and animal-originated contamination(Delcenserie et al. 2011). Apart from these new-found bacterial indicators, some fecal organic compounds such as fecal sterols and stanols could also be used to signal the fecal contamination in water. These compounds can be produced through the microbial hydrogenation of cholesterol (a dominant sterol in mammalian cells) and subsequently excreted in feces. Studies have found that the composition of sterols varies among different species due to their dietary differences, and thus the analysis of sterols could provide distinctive sterol fingerprint, which could contribute to fecal contamination source tracking(Obuseng and Nareetsile 2013; Rochelle-Newall et al. 2015).

Despite the fact that bacterial indicators can assess some level of microbial pathogen footprint in aquatic environment, their suitability for the assessment of waterborne viruses is still

debatable. It has been found that bacterial indicators do not correlate well with some of the enteric viruses, consequently, solely using FIB as a proxy for microbial water quality monitoring is inadequate. Given the inconsistent correlation between FIB species and viruses, *bacteroides fragilis* bacteriophage and coliphages (Male-specific RNA phages phages) have been proposed as surrogate viral indicators by reason of their physical and genomic similarities to enteric viruses and greater abundance in environmental water samples than that of enteroviruses(Savichtcheva and Okabe 2006).

2.4 Microbial pathogen detection

2.4.1 Traditional culture based methods

Pathogen detection and quantification are the crucial steps in the assessment of microbial water quality and health risk associated with the exposure to the disease-causing microbes. Traditional culture-based methods are based on the growth of target microorganisms on nutrient media and enumeration of replicating microbes. After incubation under proper conditions, the growth of target microorganisms can be detected visually based on turbidity change or the formation of colony or plaque in culture media. The identification and enumeration of microorganisms are supplemented with the addition of specific selective agents in culture media that enable the target microbes to develop characteristic colonial pigmentation (i.e. color or fluorescence changes). And thus, these methods are considered as relatively inexpensive and easy to operate approaches for the detection and quantification of target microorganisms. One advantage of culture based method is that sample cultivation can be performed in different formats such as petri dish, test tubes and 96-well plates. For example, apart from direct viable plate counts, most probable number (MPN) method is also used to measure the concentration of the target microorganism in water samples. A series of sequen-

tial dilutions of original water sample is inoculated into liquid culture broth for incubation, and a suite of replicates at each dilution level is performed. A statistical estimate called most probable number of the original target concentration can be calculated using the percentage of positive culture samples. MPN method allows the measurement of low concentration samples and the accuracy of estimation can be improved by altering the dilution ratio and replicate number (Woomer et al. 1990; Sutton 2010). The dilution of original water sample also mitigates the influence of sample matrix interference in direct plate count enumeration method. Moreover, membrane filter (MF) technique as an alternative procedure to MPN method is also used as means of the isolation and enumeration of target microorganisms. By coupling membrane filtration and selectiveness of growth media, this method allows the isolation and enumeration of target microorganisms.

However, culture-based methods normally require a minimum of 18-24 hrs incubation, which may lag behind in waterborne disease risk management. The accuracy and precision of culture-based enumeration methods are challenged by the selectivity of growth media and potential inhibitory effects from selective agents. The effectiveness of these methods is closely associated with the culturability of target microorganisms since some microorganisms may enter viable-but-non-culturable state as an adaptation to adverse environmental conditions (e.g. extreme temperature, irradiation, and the addition of disinfectants (Zhao et al. 2017). Consequently, to some extent, conventional cultivation methods may yield false-positive results and underestimate the concentration of the microorganisms of interest(Deshmukh et al. 2016). Despite being challenged by the culturability of microorganisms and specificity of selective media, culture-based method remains a useful approach in pathogen identification and quantification as it can provide information on viability and infectivity of target microorganisms. Furthermore, the reducing the need of complex laboratory equipment improves the analytical capacity of culture based methods in resource-poor settings, and are therefore considered as the gold standard in water quality regulation and guidelines.

2.4.2 Molecular techniques

The advent of culture-independent methods have significantly revolutionized the microbiological diagnosis. Immunoassays and nucleic acid-based techniques have expanded the spectrum of pathogen detection and dramatically shortened the detection time to hours, rather than days to weeks as is required in cultivation methods. These culture-independent methods have been proven beneficial in overcoming the limitations of traditional procedures, and extensively applied in the detection and characterization of slow-growing, difficult-to-culture, or unculturable pathogens. Immunoassays such as enzyme-linked immunosorbent assay (ELISA) have been employed for the detection of pathogens. These immunological methods are based on the principle of specific antibody-antigen interaction. Polyclonal or monoclonal antibody is used to recognize and bind to specific antigen. However, the specificity and sensitivity of these method can be affected by the density and cross reactivity of antibodies(Frampton et al. 2014). In multiplex ELISA, false-positive or false-negative results can arise from the inappropriate interactions among antibodies or closely related antigens. Nanomaterials with a high surface-to-volume ratio have been integrated with ELISA to improve its detection sensitivity (Deshmukh et al. 2016).

Many emerging nucleic acid based methods have been developed for rapid detection and quantification of pathogens. For instance, polymerase chain reaction (PCR) assays have been widely used in clinical diagnosis of pathogen causing infectious diseases. In PCR, with the prior knowledge of target DNA sequence, a pair of primers is designed to recognize the specific regions of the target sequence, and the DNA polymerase is used to assemble copies of target sequence. Many PCR primer sets have been designed for the detection of known waterborne disease agents and further optimized to achieve multiplexed pathogen detection in one reaction (i.e. multiplex PCR). Quantitative real-time PCR (qPCR) is an appealing alternative of conventional PCR which allows simultaneous detection and precise quantification of specific DNA sequences in the sample. In qPCR reaction, fluorescent dye (SYBR®

green) or dual-labelled probe (TaqMan® probes) is used to signal the ongoing DNA amplification process. The real-time monitoring of fluorescence intensity changes during PCR cycling allows the absolute DNA quantification. Because of the high specificity and sensitivity of qPCR, it has been used as a standard protocol for the robustness evaluation and data validation in the development of novel nucleic acid based analytical methods. Furthermore, the viability PCR has been designed to circumvent the disadvantage of traditional PCR assays, that is, the inability to discriminate between viable and non-viable cells due to the persistence of DNA in the environment after cell death. The strategy relies on the integration of traditional PCR reaction and pretreatment of samples with nucleic acid intercalating dyes such as propidium monoazide (PMA). The intercalating dye can penetrate membrane compromised cells and is capable to covalently crosslinked to DNA upon exposure to bright light, resulting in a stable dye-DNA complex that cannot be amplified by PCR(Quijada et al. 2016).

Advances in genetic analysis have resulted in the expansion of the capacity of nucleic acid based methods from single target detection to simultaneous identification and characterization of multiple targets. Next generation sequencing (NGS) is an emerging approach for pathogen detection and profiling microbial community in aquatic environment. In contrast to multiplex PCR assay, NGS is capable of delivering massive parallel analysis of DNA sequences and in-depth genomic information without prior sequence knowledge on target pathogens, which allows identification of novel pathogens in environmental samples. NGS accelerates the process of genomic information acquisition, however, processing and interpretation of large volume of generated sequencing data remains a hurdle in its routine diagnostic applications as downstream computational and mathematical tools and well-trained personnel are required (Moorcraft et al. 2015). In addition, functional nucleic acid such as aptamers have been used for the development of nucleic acid amplification-free methods for pathogen detection. Aptamers are specific nucleic acid sequences (single stranded DNA or RNA ligands) which can specifically recognize and bind to various chemical and biological

targets, and therefore are considered as chemical antibody. Aptamers are isolated through an iterative screening process called systematic evolution of ligands by exponential enrichment (SELEX) which involves large scale screening of random oligonucleotide libraries. And thus, aptamers show high affinity and specificity for binding to their targets. In comparison with antibodies, aptamers show relative higher binding efficacy as the specific binding including not only large molecules such as proteins and cells but also small molecules such as nucleotides and amino acids (Alizadeh et al. 2017). Besides, the higher surface density of aptamers also improve the binding efficiency. However, because of the complexity in high affinity aptamer screening and associated sample preparation and detection processes, the routine use of aptamer-based methods in the pathogen detection is still challenging (Teng et al. 2016).

2.4.3 Integrated microfluidic molecular diagnostics

Microfluidic technologies have gained attention in improving the performance of molecular diagnostic assays and applicability of point-of-care diagnostic devices as it has the potential to miniaturize the analytical devices, simplify the complex experimental procedures, and achieve automatic analysis of samples. Moreover, microfluidic devices also permit low reagent consumption and cost reduction (Schuler et al. 2016; Park et al. 2017). For example, "Lab on a chip" (LOC) microfluidic devices have been successfully employed in single-copy nucleic acid detections to achieve on-chip digital quantification of DNA (Fu et al. 2017; Ding et al. 2017) and multiplexed digital PCR (Bian et al. 2015; Chen et al. 2017); Furthermore, the integration between PCR reaction and microfluidic technologies offers advantages over conventional PCR assay by providing better quantitative results with improved precision and reproducibility (Hall Sedlak and Jerome 2014). In previous study, a microfluidic disposable chip was developed for digital PCR. The geometry design ensures the is capable of partitioning 50 μl PCR sample into 1-million 50 pl droplets in less than 10 mins. Each droplet

functions as an individual PCR reaction. By measuring the percentage of PCR positive droplets after the PCR cycling, the quantity of original DNA templates can be quantified statistically without relying on a standard curve. This digital PCR system delivers high sensitive DNA quantification results, with a detection limit of 10 copies/50 μl PCR reaction (Hatch et al. 2011b). Moreover, a droplet digital PCR (ddPCR) system from Bio-Rad ® has been commercialized. It is capable of parallel quantification of microbial pathogens within a few hours and theoretically, it could reach a lower detection limit of 1copy/reaction. However, the current ddPCR system consists of a series of sophisticated instrumentation that function separately, which makes it cost-prohibitive for onsite water quality assessments in resource-limited regions. Therefore, it is necessary to develop alternative system for fast, sensitive, and cost-efficient detection and quantification of waterborne pathogens.

2.4.4 Loop-mediated isothermal amplification (LAMP)

Loop-mediated isothermal amplification (LAMP) is an emerging DNA amplification method that can amplify DNA under constant temperature (65°C-72°C), and the time required for the amplification process is ranging from 30 min to 1h (Notomi et al. 2000). A set of 6 primers recognizing 8 distinct regions of target DNA provides LAMP higher specificity than PCR assay. Besides, the addition of a pair of loop primers offers additional starting points for DNA synthesis, and consequently accelerates the amplification process. However, LAMP only yields binary results (i.e. positive or negative). Therefore, converting it to a quantitative method may provide significant potential for it to be further optimized for field deployment. The combination of binary outcome and microfluidic droplet system may be a feasible way. A microfluidic disposable cartridge (DropChip) has been developed for digital droplet LAMP (ddLAMP) (Schuler et al. 2016). This ddLMAP system is capable to generate high sensitive DNA quantification results, however, the quantification is based on scanning the fluorescence signal exerted from the 5' fluorescently labeled forward inner

primer (FIP). Apart from the requirement of a microarray scanner, labeling primer with a quencher for fluorescence generation also increases the final cost, which may hinder its further applications in environmental water assessment. In addition, the amplification reaction is relatively sensitive to changes in the percentage of labeled FIP, since excessive labeled FIP could inhibit LAMP reaction. Therefore, more precise and laborious laboratory work is required for this method.

Method		Advantages	Limitations
Nucleic acid based	PCR	Specific, sensitive, qualitative	Sensitive to PCR inhibitors; cannot distinguish between viable and non-viable cells
	qPCR	Specific, sensitive, simultaneous detection and quantification	High cost, absolute quantification relies on standard curve
	multiplex PCR	Specific, sensitive, Simultaneous multiple target detection	Primer design is crucial
	LAMP	Specific, sensitive, isothermal amplification, low cost, higher inhibitor tolerance	Not quantitative
	ddPCR	Specific, sensitive, quantitative, rapid	High cost
	NGS	Specific, sensitive, detect unknown species	High cost, complex data analysis
	Aptamers	Specific, sensitive	Complex aptamer screening process
Immunological based	ELISA	Specific, examine multiple samples simultaneously, detect bacterial toxins	Low sensitivity, false negative or false positive results

Table 2.2: A summary of advantages and limitations of pathogen detection methods

Chapter 3

Material and Methods

3.1 Culture conditions and sample preparation

Bacterial stain used in this project was from the culture collection at the Applied microbiology laboratory, University of California, Irvine. *Enterococcus Faecalis* was used for LAMP assay optimization and sensitivity evaluation, as well as the demonstration of the operation of the microfluidic chip.

To prepare bacterial sample, a loopful frozen glycerol-stored *Enterococcus Faecalis* (ATCC 29212) was scraped off and inoculated in 5 ml Luria-Bertani (LB) broth for liquid cell culture. After overnight incubation at 37°C in a shaking-incubator, 0.1 ml bacteria cell solution was transferred onto a LB agar plate via streak plate method followed by 18 hrs incubation at 37°C in incubator. The streaked LB agar plate was stored at 4°C and was used as stock culture in this study. Before each LAMP test, a fresh cell suspension was prepared. Additionally, to estimate the number of *E. faecalis* in liquid culture, a series of ten-fold dilutions of original cell solution were prepared by mixing 0.1 ml cell solution with 0.9 ml distilled water, and the concentration of the diluted cell solutions was calculated

with the final unit of Colony Forming Units per ml (CFU/ml), according to the instruction of EPA method 1600, mEI membrane filtration method (U.S. EPA, 2002). Besides, the availability and sensitivity of LAMP assay were evaluated using *E. faecalis* spiked water samples (i.e. seawater, San Diego creek water and secondary effluent from Orange County Sanitation District). Serial ten-fold dilutions of spiked water samples were prepared with the final concentration of 200 to $2 \times 10^7 CFU/ml$. A negative control was included in each dilution series (i.e. water sample without the addition of bacterial cell solution).

3.2 LAMP reagents preparation

LAMP primer sets designed previously (Kato et al. 2007) for targeting azoA gene of *E. faecalis* were employed in this study. LAMP reaction was conducted with three pairs of primers including inner primers (FIP and BIP), outer primers (F3 and B3) and loop primers (LF and LB). The LAMP amplicon size was 220 bp. The sequences of primers were shown in Table 3.1.

To prepare the LAMP reaction mix, DNA sample was crudely extracted using bead-beating method. A total of 200 μl of each *E. faecalis* spiked water sample was transferred into sterile screw-cap Eppendorf tubes with the addition of 0.5 g of 0.5 mm silica beads (BioSpec Products, OK, USA). Subsequently, the cells were disrupted using vortex mixer at the maximum speed for 6 min. After the centrifugation under $10,000 \times g$ for 1 min, the supernatant was obtained as the DNA template in LAMP reaction. The extracted *E. faecalis* DNA sample was denatured by heating at 85°C for 2 min and immediately placed on ice. After denaturation, 2 μl of DNA sample was mixed with LAMP reagents according to the protocol of WarmStart®LAMP Kit (New England Biolabs (NEB), MA, USA). The LAMP reaction mix in a total volume of 25 μl contained a 1X WarmStart LAMP Master Mix (consisting of Bst 2.0 WarmStart DNA Polymerase and LAMP buffer solution), 1X fluorescent dye (NEB,

MA, USA), 1.6 μM each of FIP and BIP, 0.2 μM each of F3 and B3, 0.8 μM each of LB and LF, 1 $\mu g/\mu l$ Bovine serum albumin (BSA) (Sigma-Aldrich, USA), and 2 μl of DNA sample. All concentrations refer to the final concentrations in LAMP reaction mix.

Primer	Sequence
F3	5'-GCCGGAAATCGATGAAGA-3'
B3	5'-TCCAGCAACGTTGATTGT-3'
FIP	5'-CACTTTTTGTTGTTGGTTTTCGCTTTATTATCTGCTTGGGGTGC-3'
BIP	5'-ATCTGCAGACAAAGTAGTAATTGCTCCAAGCTTTTAAGCGTGTC-3'
LoopF	5'-AAATGCTGCGCCAGCTCG-3'
LoopB	5'-TCCAATGTGGAACTTAAACGTACC-3'

Table 3.1: Oligonucleotide Primers for *Enterococcus Faecalis* LAMP

3.3 Microfluidic chip design

Hatch, Andrew C., et al developed a microfluidic device for droplet based digital PCR. In this study, PCR reaction was replaced with LAMP reaction to simplify the experimental procedure, and the geometric design was employed in this study. Microfluidic chip was reproduced with the permission of Hatch, Andrew C., et al. The microfluidic chip was designed using AutoCAD software (Autodesk Inc., San Rafael, CA), as shown in Figure 3.1a. A flow-focusing geometry was used for initial parent droplet ($\sim 11nl$) generation. When the parent droplet reaches the bifurcation junction, as the fluidic resistance of two daughter channels are the same, an angle of 45 permits symmetric breakage of droplet (Simon and Lee 2012). As a result, the parent droplet can be evenly split into 2 daughter droplets (as illustrated in figure 3.1b). A repeating bifurcation design allows seven consecutive splitting of parent droplets by which a single parent droplet is split to 128 daughter droplets (figure 3.1c). The combination of flow-focusing droplet generation and consecutive bifurcation junctions ensures robustly large quantity of monodispersed droplet generation and high frequency of LAMP reaction sample encapsulation. Moreover, two vertical support strips in droplet

viewing chamber were used to stabilize chamber structure and to prevent chamber collapse due to chip assembly and structural distortion caused by LAMP sample loading and on-chip heating.

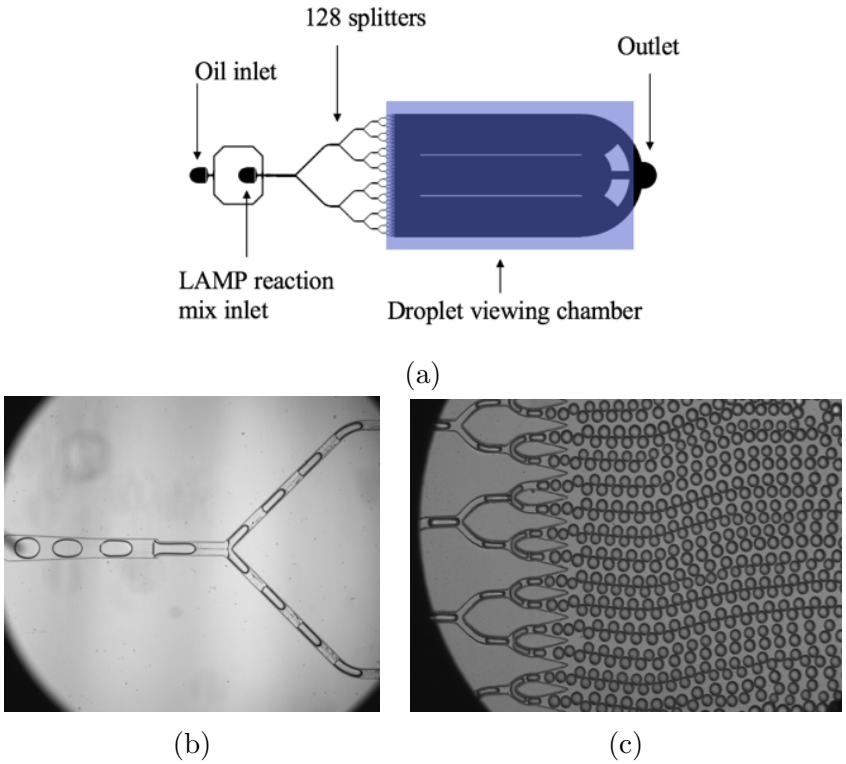

Figure 3.1: (a) Schematic illustration of microfluidic chip design. (b) Bifurcation junction. (c) Consecutive droplet fission.

The chip is composed of two inlets (for oil and LAMP sample loading), flow-focusing droplet generator, 128 droplet splitters, and a droplet viewing chamber. At the first Y-shaped bifurcation junction, a parental channel of width 240 mm split into two daughter channels of the same length with 45 bifurcation angel, a$\sqrt{2}$ width reduction was applied from bifurcation junctions 2 to 6.

3.4 Microfluidic chip fabrication

The polydimethylsiloxane (PDMS)-glass hybrid microfluidic chips were fabricated through standard soft lithography processes. PDMS is a widely used material in microfluidic device fabrication (Tang and Whitesides 2010), and soft lithography is considered as a simple and cost-efficient chip fabrication procedure, which leads to the benefit of lower cost of droplet LAMP assay (Shih and Lee 2016). Negative-tone epoxy photoresist SU-8, 2050 (MicroChem, USA) was spin-coated on 3-inch silicon wafer to form a single-height microfluidic master (mold) with a thickness of 80 mm in a clean room. Sylgard-184 PDMS (Dow Corning), a two-part component kit with a 10:1 ratio (v/v) of silicone elastomer base to curing agent, was used for the production of PDMS replica. The liquid PDMS prepolymer was poured over the master and cured in an oven for 4-6 hrs at 60°C, then peeled from the master. After the inlets and outlets were cored, the microfluidic channels were sealed by bonding the PDMS replica to a 1.06 mm thick $75mm \times 25mm$ glass slide, and another 1.06 mm glass slide was bonded on the top of PDMS right above the droplet viewing chamber. The glass-PDMS-glass bonding was achieved via air plasma treatment (Harrick Plasma, USA), which relies on the oxidation of interfaces. Since the oxygen plasma treatment reduced the PDMS hydrophobicity, placing the entire chip in a 120°C oven for 24 hrs can return PDMS to its original hydrophobic state (Hatch et al. 2011b; Tang and Whitesides 2010). Figure 3.2 shows the sandwich structure of the droplet LAMP chip.

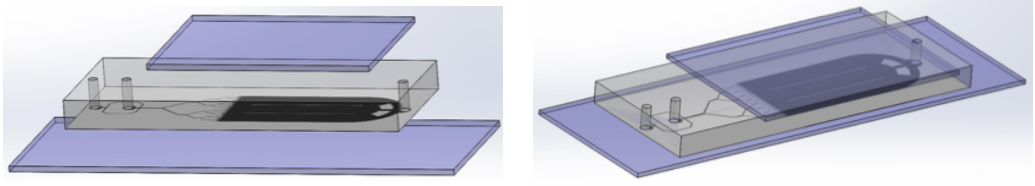

Figure 3.2: Schematic view of the droplet LAMP chip. Top and bottom layers were glass slides and the middle layer was patterned PDMS

3.5 Microfluidic chip operation

LAMP reaction sample encapsulation was achieved using heavy mineral oil (Sigma-Aldrich) with 3% w/w Abil EM 90 (Degussa/Goldschmidt) and 0.1% w/w Triton X-100 (Sigma-Aldrich) as stabilizing surfactants. To generate droplets, fresh prepared LAMP reaction sample and oil were stored in two screw-cap tubes, where microbore tubings (Tygon, Sigma) were mounted to ensure fluidic connection between off-chip sample reservoirs and microfluidic device. External pneumatic pressure pump controlled by a scalable pressure modulator was used to pressurize and inject LAMP reaction sample and oil into the chip from two inlets respectively. Typically, the system operational pressure was 12-13 psi. For droplet generation, the operational pressure of aqueous and oil phases was 1.6 psi and 2.6 psi, respectively, resulting in the droplet generation frequency of 0.384 kHz and 61.5% water/oil (w/o) volume ratio. Based on previous study, the water/oil volume ratio is within the preferable range for single layer droplet close-packing configuration (Hatch et al. 2011a). Subsequently, generated droplets were collected in a $12.8mm \times 19.2mm$ droplet viewing chamber. When the chamber was filled with droplets, the entire chip was placed on a heating block and incubated at 65°C for 30 min.

3.6 Droplet image acquisition and analysis

During droplet generation, the microfluidic chip was placed on the Nikon 100-S inverted microscope, and a high-speed camera (V310 Phantom, Vision Research) was connected to the microscope for monitoring and recording the droplet generation processes at flow-focusing region and subsequent bifurcation junctions. After incubation, because of the presence of fluorescent dsDNA binding dye, the LAMP positive and negative droplets can be differentiated based on fluorescence intensity. Microscopic observations of fluorescence were made using

Olympus IX71 fluorescence microscope, the fluorescent droplets were imaged using a high resolution monochrome cooled CCD camera (ORCA-D2, Hamamatsu). An image processing software ImageJ (NIH) was used to measure droplet size, analysis fluorescence intensity, and quantify fluorescent droplets from captured droplet images. Droplet data was then fit to a Poisson distribution for cell loading concentration calculation. Given the volume of droplet, the concentration of *E. faecalis* in LAMP sample could be calculated statistically according to the following equation:

$$C = -\frac{\ln(1 - \frac{N_p}{N_{total}})}{V_{droplet}}$$

where N_{total} is the total number of droplets in each image, N_p is the number of positive droplets, and N_p/N_{total} is the fraction of positive droplets, $V_{droplet}$ is the droplet volume (μl).

Chapter 4

Results and discussion

4.1 Influence of incubation conditions on LAMP sensitivity

LAMP assays were evaluated in the format of traditional PCR tube using WarmStart®LAMP Kit (New England Biolabs (NEB), MA, USA). Bst polymerase was used in the LAMP reagent formulation. With a unique strand replacement activity, Bst polymerase permits rapid and continuous isothermal amplification of target DNA. 65°C was considered as the optimum temperature of Bst polymerase in previous studies (Notomi et al. 2000; Chander et al. 2014). In this study, LAMP reaction was conducted with incubation temperature varying from 63°C to 72°C. A reduction in amplification efficiency could be observed when sample incubation temperature fell below 65°C or exceeded 70°C. Therefore, to ensure the highest enzyme activity during LAMP reaction, 65°C incubation temperature was selected in this study. Apart from the optimization of reaction temperature, reduction of overall incubation time without sacrificing target detection sensitivity may also improve the efficiency of LAMP assay. Thus, to determine the optimal incubation time, LAMP performance was evaluated

by comparing the limit of detection after different incubation time. A serial dilution of DNA sample extracted from *E. faecalis* fresh overnight culture was tested and three LAMP replicates were performed per dilution. Table 3.1 illustrates the comparison of LAMP results after four different incubation time. 25 min of incubation was sufficient to perform LAMP amplification only in relatively high concentration samples. As shown in table 3.1, the LAMP positive result was undetectable in samples with a lower concentration (i.e. 4-40 CFU/reaction) when 25 min of incubation was applied. Although the diminution of detection sensitivity was not observed with incubation over 30 min, the chance of non-specific background amplification was increased, resulting in false-positive results in negative control tests (as shown in Table 4.1). Overall, 30 min was chosen as the optimal incubation time for the subsequent droplet LAMP assays.

E. faecalis concentration (CFU/reaction)		40,000	4,000	400	40	4	0.4	Negative control
65°C	20 min	+	+	+	+	-	-	-
	30 min	+	+	+	+	+	-	-
	45 min	+	+	+	+	+	+ /-	+ /-
	60 min	+	+	+	+	+	+ /-	+ /-

Table 4.1: Influence of incubation time on LAMP sensitivity

+: clearly visible LAMP positive results; -: LAMP negative. Amplified products were verified by electrophoresis on 2% agarose gels, and the display of a characteristic ladder pattern of bands was considered as positive LAMP products.

4.2 Droplet stability and uniformity

4.2.1 Influence of oil and surfactant composition

Droplet stability plays a significant role in droplet based digital molecular diagnostics. To ensure stable LAMP reaction sample encapsulation, four different oil-surfactant compositions were compared on the basis of their performance during water-in-oil emulsification and on-chip incubation processes. Four different types of LAMP sample (i.e. LAMP reagents with *E. faecalis* pure culture, *E. faecalis* spiked seawater, San diego creek water, and secondary effluent) were used to evaluate the chemical compatibility of LAMP assay with emulsification reagents and the droplet thermal-stability during on-chip incubation. Table 4.2 listed all of the oil and surfactant compositions attempted in this study. The combination of HFE7500 with Pico-Surf ^{TM} 1 surfactant had been successfully used as carrier fluid in previous droplet microfluidics studies (Schuler et al. 2015; Rhee et al. 2016); however, unlike the previous works, the droplets containing LAMP samples were extremely vulnerable to internal pressure change in sample loading tubings and microchannels, resulting in massive droplet coalescence in droplet viewing chamber in droplet generation process. Moreover, noticeable droplet shrinkage caused by sample evaporation was also observed during on-chip incubation. By comparing the overall droplet integrity, heavy mineral oil with 3% Abil EM 90 and 0.1% Triton X-100 as surfactants was selected as the optimal oil and surfactant composition in droplet-scale LAMP assay. It guarantees comparatively high chemical compatibility with various LAMP samples and high thermal-stability during continuous heating at 65°C as apparent droplet deformation and breakups were not observed during the incubation process.

Interfacial tension can significantly affect the performance of droplet fission and is crucial for maintaining droplet thermal stability (Tadros 2013). High interfacial tension can hinder the continuous droplet fission through bifurcating microchannels and may induce droplet coalescence during on-chip incubation. However, low interfacial tension may pinch off the droplet

tail and tend to produce relatively large droplets with undesired satellite droplet in between. The combination of 3% Abil EM 90 and 0.1% Triton X-100 successfully prevents droplet coalescence during emulsification and allows the existence of proper interfacial tension gradients, which is instrumental in stabilizing the interface between two droplets. Furthermore, Abil EM 90 was used as a competitive interface binding agent to reduce polymerase adsorption to droplet surface. The reduction of adsorption of DNA and polymerase was further facilitated by the addition of BSA, an inactive protein, in LAMP sample phase(Pandit et al. 2015).

Oil	Surfactant	Droplet stability	
		Before incubation	After incubation
Heavy mineral oil	3 wt% Abil EM 90&	stable	stable
Light mineral oil	0.1 wt% Triton-x-100	stable	partial coalescence
HFE 7500	0.1 wt% Pico-Surf ^{TM} 1	unstable	coalescence
	3 wt% Pluronic®F-68	unstable	coalescence
Biorad oil	-	stable	coalescence

Table 4.2: Effects of oil-surfactant compositions on the stability of droplet

4.2.2 Influence of PDMS permeability and chip deformation

PDMS is commonly used in microfluidic device fabrication, however, due to the porosity of PDMS, droplet evaporation during incubation may occur, which may alter the reagent concentration in droplet, and further inhibit the DNA amplification reaction. Because of the low water vapor permeability of glass, implanting a vapor barrier layer in PDMS above the droplet incubation chamber was used to minimize the adverse impact of air permeability of PDMS in previous studies (Heyries et al. 2011; Hatch et al. 2011b). In this study, the glass embedment in PDMS step was simplified by directly bonding a glass slide on the outside of the upper surface of PDMS layer. This glass-PDMS-glass sandwich structure provided a full coverage of the droplet viewing chamber. Two glass slides not only served as effective permeation barriers for sealing the PDMS chamber from both sides, but also enhanced the

structural strength of microfluidic chip and to some extent eliminated the occurrence of the chip deformation at elevated temperature. Figure 4.1a shows the droplets condition after 30 min incubation in the original PDMS-glass chip. Without top glass slide assembled, air may permeate into the chip. The explosion of air bubble may alter the internal pressure of droplet chamber, resulting in morphological changes of droplet. Droplet loss and oversized droplet formation could be observed. Moreover, without proper support, undesired chip distortion and chamber collapse caused by PDMS deformation during continuous heating may also attribute to droplet merging and breakups. Figure 4.1b shows the droplets condition using sandwich structured chip. Droplet were stable after incubation, and a single layer of close packed lattice pattern could be obtained.

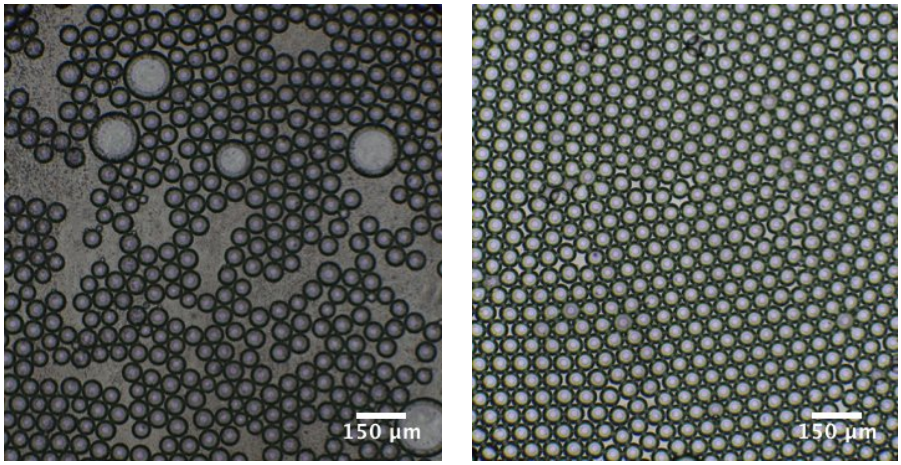

(a) Chip without top glass slide (b) Chip with top glass slide.

Figure 4.1: A comparison of droplet size and density after 30 min on-chip incubation with and without a top glass slide assembled.

Overall, the stability and uniformity of droplet are effected by a combined effect of LAMP sample emulsification oil and chip fabrication material. By comparing the overall performance of different combinations of oil and chip configuration, the combination of heavy mineral oil and sandwich structure was selected. With the chip geometry design, monodispersed droplets could be generated with a good monodispersity and the CV value of 3.7%. The average diameter of the droplets was 55 μm (for details see Appendix A).

4.3 Sensitivity of droplet LAMP assay

4.3.1 Influence of DNA denaturation on droplet LAMP

Previous study reported that in digital LAMP assay DNA denaturation prior to LAMP sample emulsification could improve the DNA accessibility to LAMP primers and improve the accuracy of target quantification (Schuler et al. 2016). In this study, two aliquots of DNA sample extracted from the same *E. faecalis* pure culture were used to evaluate the influence of DNA denaturation on droplet LAMP. As shown in Figure 4.2, the denatured DNA sample showed threefold increase in the percentage of positive droplets.

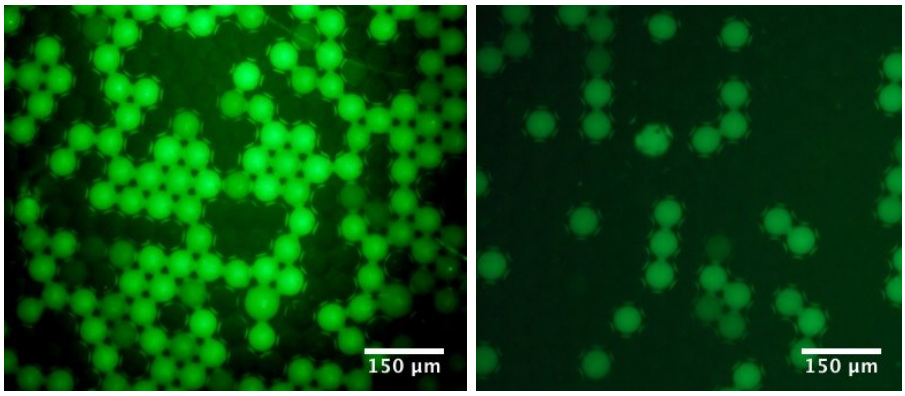

(a) With DNA denaturation, 43.1% of droplet fluoresced

(b) Without DNA denaturation, 13.8% of droplet fluoresced.

Figure 4.2: Fluorescence image of droplet LAMP.

4.3.2 Sensitivity of Droplet LAMP for *E. faecalis* quantification

The sensitivity of *E. faecalis* quantification using droplet LAMP assay was evaluated using the DNA sample extracted from a ten-fold serial dilution of *E. faecalis* fresh overnight culture (the corresponding *E. faecalis* concentration ranged from with 4 to 4×10^4 CFU/reaction). Image J was used for droplet image processing and fluorescent droplet quantification (see

details in Appendix B). The calculated concentration of *E.faecalis* was compared with the viable plate counts. The representative images of droplet LAMP chip after incubation were shown in Figure 4.3. As the *E. faecalis* concentration increases, a corresponding increase in the percentage of LAMP positive droplets could be observed.

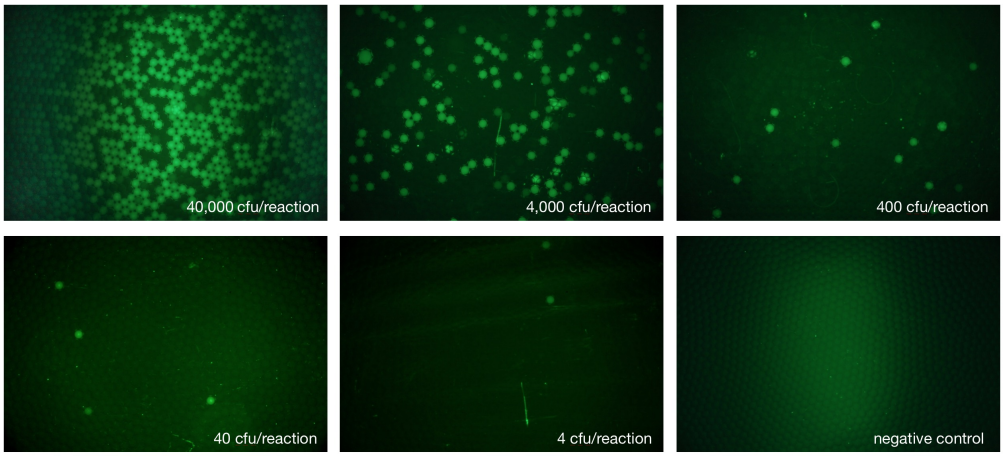

Figure 4.3: Droplet LAMP results with a serial dilution of *E. faecalis* ranging from 4 to 4×10^4 CFU/reaction. The subcaptions of the images were the expected *E. faecalis* concentration obtained by viable plate counts.

The *E. faecalis* concentration calculated using droplet data was compared with colony plate counts for droplet LAMP data validation. A comparison of droplet LAMP results and viable plate counts can be seen in Figure 4.4. The results showed a positive log linear correlation ($R^2 = 0.9819$) between calculated concentration and the expected concentration of *E. faecalis*. The discrepancy occurred at the high concentration may related to the limitation on the dynamic range of the droplet assay as the upper limit of detection of droplet LAMP is decided by the number of droplet generated per reaction. The relatively large error between expected and calculated concentration at the lower concentration range was also observed, which may because of the loss of DNA sample during DNA preparation. Moreover, the on-chip LAMP amplification efficiency and fluorescence signal to background noise level may also affect the fraction of positive droplet. Since the fraction of positive droplet is positively correlated to the calculated sample concentration, the variation on the ratio of positive to total number of droplet may further affect the accuracy of sample concentration calculation.

Furthermore, droplet image selection bias may also contribute to the variation between the value derived from droplet LAMP and that from culture method. Image capture of large field of view is essential to the accuracy and precision of droplet data analysis as a relative large number of droplet could be captured each time. Because of the limitation of camera's field of view, multiple regions within the chamber were imaged to give a better representation of the entire droplet viewing chamber. However, a bias was introduced when combining the quantification data from several captured images. For an expected concentration of 4 CFU/reaction, one of the selected region may show 2 positive droplets, which would provide a relatively higher percentage of positive droplet. However, the real percentage of positive droplet for the entire chamber may be much lower. Therefore, the relationship between the degree of image overlap and number of image captured within each chip played an important role in droplet data analysis.

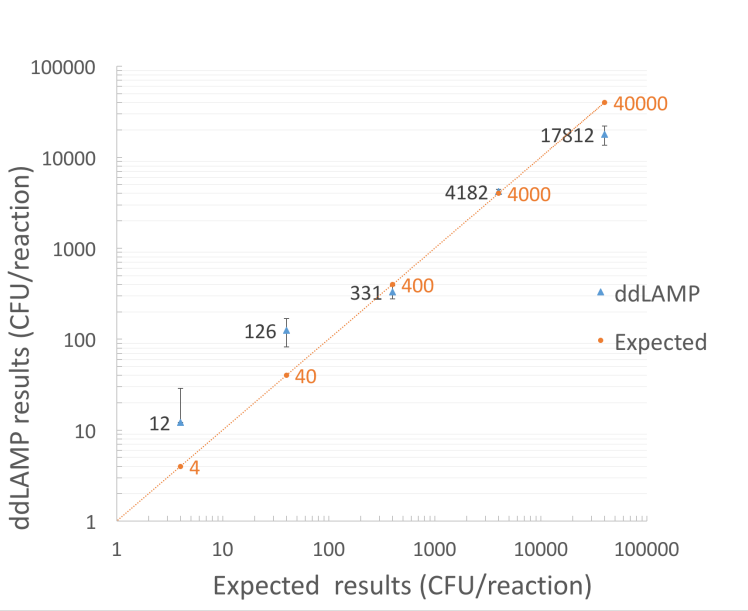

Figure 4.4: Comparison of the droplet LAMP results and viable plate counts (data was plotted on logarithmic scales).

4.3.3 Availability of LAMP assay

To evaluate the availability and determine the limit of detection of droplet LAMP assay for *E. faecalis* quantification, *E. faecalis* pure culture, *E. faecalis* spiked seawater, San Diego creek water, and secondary effluent were selected as experimental water samples. Ten-fold serial dilutions of each type of water sample were first tested in triplicates using conventional LAMP method in test tube, and subsequently droplet LAMP assay was performed on the same water samples at each dilution. Table 4.3 shows the availability and sensitivity tests performed with traditional LAMP. Positive LAMP results could be observed in all of the tested water samples, and the lower limit of detection were near the order of 4 CFU/reaction in *E. faecalis* pure culture.

Water samples	E.faecalis concentration (CFU/reaction)				
	40,000	4,000	400	40	4
E.faecalis pure culture	3(3)	3(3)	3(3)	3(3)	3(3)
E.faecalis spiked seawater	2(3)	1(3)	0(3)	0(3)	0(3)
E.faecalis spiked San Diego creek water	3(3)	3(3)	1(3)	1(3)	0(3)
E.faecalis spiked secondary effluent	3(3)	3(3)	1(3)	0(3)	0(3)

Table 4.3: Results of the availability and sensitivity tests performed with traditional LAMP assay

It should be noted that the detection limit of LAMP decreased as the complexity of sample matrix increased. Since DNA sample preparation mainly relied on mechanical procedures (i.e. bead beating and centrifugation), LAMP inhibitors orientating from the sample matrix may not be efficiently removed from DNA sample. To some extent, the presence of impurities in crude extract DNA sample may affect the enzymatic activities and further hinder the assay performance and effectiveness in certain events. In addition, the DNA amplification efficiency and sensitivity of LAMP assay could also be affected by the quantity of DNA templates. As bead beating was used for crude DNA extraction, the DNA sample recovery rate was subject to the degree of DNA adsorption to the surface of silica beads. Certain dissolved impurities in

water sample may alter the affinity between silica beads and DNA molecules. The influence of DNA sample quality and quantity on droplet-scale LAMP was also observed. Figure 4.4 shows the performance of droplet LAMP on *E. faecalis* spiked environmental samples. In comparison with the quantification results of *E. faecalis* pure culture, droplet LAMP showed a comparatively narrower effective range when high-complexity environmental matrices were introduced in reaction mixture. Valid droplet quantification data could not be obtained when a lower concentration sample was used (as can be seen in Figure 4.5a and 4.5b, no available data in low concentration region). As the quantity of DNA template decreases during consecutive sample dilution, the percentage of LAMP positive droplet is expected to decreases synchronously. However, unlike the results of *E. faecalis* pure culture sample, no LAMP positive droplet could be observed when sample concentration decreased below the order of 400 CFU/reaction. Furthermore, even the positive droplet could be observed in high concentration samples, the quantification data of droplet LAMP was several orders of magnitude lower than the expected value. The asynchronous change of the percentage of positive droplet and sample concentration may be because of the persistence of LAMP inhibitor in extracted DNA sample or the undesired template DNA loss during DNA sample preparation. Therefore, to improve the sensitivity and applicability of droplet LAMP, further DNA purification should be conducted after mechanical cell lysis.

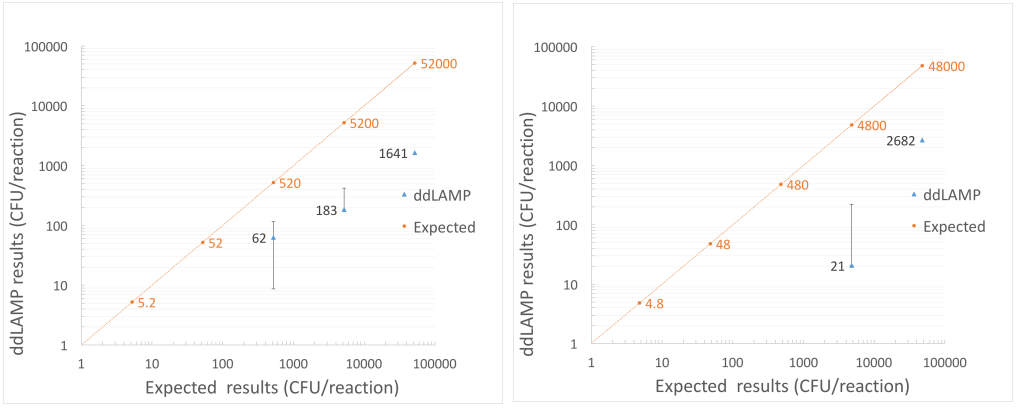

(a) *E.faecalis* spiked OCSD secondary effluent

(b) *E.faecalis* spiked San Diego Creek water

Figure 4.5: The performance of droplet LAMP on samples of different matrices

Chapter 5

Conclusion and future directions

In this study, we have demonstrated a promising approach for the specific detection and rapid quantification of *Enterococcus. Faecalis*, which was achieved by combining isothermal nucleic acid amplification assay and partitioning of reaction sample into several thousands of droplets in a water-in-oil emulsion on a single lateral flow microfluidic device. The platform setup simplifies the reaction sample preparation and operational processes and improves the efficiency of *E. faecalis* quantification procedures. The integration of flow-focusing geometry and a series of consecutive bifurcating microchannel delivers the high throughput production of monodispersed emulsion droplets. The combination of heavy mineral oil with 3% Abil EM 90 and 0.1% Triton X-100 shows high chemical compatibility with different environmental water samples. The glass-PDMS-glass chip configuration effectively prevents undesired droplet loss and maintains droplet integrity during on-chip incubation. The addition of fluorescent dye allows the visual discrimination between LAMP positive and negative droplets, and works in conjunction with droplet image recognition software to achieve a semi-automated conversion from fluorescence signal to quantitative droplet data. Although the sensitivity of droplet LAMP quantifying target microorganism in water sample is subject to the purity of DNA sample and the camera's field of view at current stage, the droplet

LAMP assay still shows promise to become a rapid diagnostic tool in the field of pathogen indicators and pathogen detection and quantification. For future research, different types of beads and the associated binding efficiency of the DNA to bead surface will be evaluated to improve the recovery and quality of DNA extracted using mechanical cell lysis. In addition, alternative pump systems (e.g. handheld or multi-channel pump) will be tested to further simplify the droplet generation process and to investigate the potential of droplet LAMP in parallel detection and quantification of multiple samples. A smartphone camera based fluorescence imaging system and associated image processing application will be integrated into current system to achieve fully automated droplet data quantification, which may also increase the practicability of droplet LAMP assay in resource-limited settings. Based on aforementioned optimization, we envision the final system to be an automated "sample in, result out" system for onsite pathogen detection and quantification.

Bibliography

N. Alizadeh, M. Y. Memar, S. R. Moaddab, and H. S. Kafil. Aptamer-assisted novel technologies for detecting bacterial pathogens, 2017. ISSN 19506007.

K. L. Anderson, J. E. Whitlock, J. Valerie, and V. J. Harwood. Persistence and Differential Survival of Fecal Indicator Bacteria in Subtropical Waters and Sediments Persistence and Differential Survival of Fecal Indicator Bacteria in Subtropical Waters and Sediments. *Applied and environmental microbiology*, 71(6):3041–3048, 2005. ISSN 0099-2240. doi: 10.1128/AEM.71.6.3041.

X. Bian, F. Jing, G. Li, X. Fan, C. Jia, H. Zhou, Q. Jin, and J. Zhao. A microfluidic droplet digital PCR for simultaneous detection of pathogenic Escherichia coli O157 and Listeria monocytogenes. *Biosensors and Bioelectronics*, 74:770–777, 2015. ISSN 18734235. doi: 10.1016/j.bios.2015.07.016.

X. Bonjoch, E. Ballesté, and A. R. Blanch. Multiplex PCR with 16S rRNA gene-targeted primers of Bifidobacterium spp. to identify sources of fecal pollution. *Applied and Environmental Microbiology*, 70(5):3171–3175, 2004. ISSN 00992240. doi: 10.1128/AEM.70.5.3171-3175.2004.

L. Carvajal-Vélez, A. Amouzou, J. Perin, A. Maïga, H. Tarekegn, A. Akinyemi, S. Shiferaw, M. Young, J. Bryce, and H. Newby. Diarrhea management in children under five in sub-Saharan Africa: Does the source of care matter? A Countdown analysis. *BMC Public Health*, 16(1), 2016. ISSN 14712458. doi: 10.1186/s12889-016-3475-1.

Y. Chander, J. Koelbl, J. Puckett, M. J. Moser, A. J. Klingele, M. R. Liles, A. Carrias, D. A. Mead, and T. W. Schoenfeld. A novel thermostable polymerase for RNA and DNA loop-mediated isothermal amplification (LAMP). *Frontiers in Microbiology*, 5(AUG), 2014. ISSN 1664302X. doi: 10.3389/fmicb.2014.00395.

C. Chen, P. Liu, X. Zhao, W. Du, X. Feng, and B. F. Liu. A self-contained microfluidic in-gel loop-mediated isothermal amplification for multiplexed pathogen detection. *Sensors and Actuators, B: Chemical*, 239:1–8, 2017. ISSN 09254005. doi: 10.1016/j.snb.2016.07.164.

V. Delcenserie, F. Gavini, B. China, and G. Daube. Bifidobacterium pseudolongum are efficient indicators of animal fecal contamination in raw milk cheese industry. *BMC Microbiology*, 11, 2011. ISSN 14712180. doi: 10.1186/1471-2180-11-178.

R. A. Deshmukh, K. Joshi, S. Bhand, and U. Roy. Recent developments in detection and enumeration of waterborne bacteria: a retrospective minireview, 2016. ISSN 20458827.

Y. Ding, J. Choo, and A. J. DeMello. From single-molecule detection to next-generation sequencing: microfluidic droplets for high-throughput nucleic acid analysis. *Microfluidics and Nanofluidics*, 21(3), 2017. ISSN 16134990. doi: 10.1007/s10404-017-1889-4.

EPA. Recreational Water Quality Criteria. *U. S. Environmental Protection Agency*, pages 1–69, 2012. doi: 820-F-12-058.

D. Ferguson and C. Signoretto. Chapter 17: Environmental Persistence and Naturalization of Fecal Indicator Organisms. In *Microbial Source Tracking: Methods, Applications, and Case Studies*, pages 379–397. 2011. ISBN 978-1-4419-9385-4. doi: 10.1007/978-1-4419-9386-1. URL http://link.springer.com/10.1007/978-1-4419-9386-1.

J. P. Frampton, J. B. White, A. B. Simon, M. Tsuei, S. Paczesny, and S. Takayama. Aqueous two-phase system patterning of detection antibody solutions for cross-reaction-free multiplex ELISA. *Scientific Reports*, 4, 2014. ISSN 20452322. doi: 10.1038/srep04878.

Y. Fu, H. Zhou, C. Jia, F. Jing, Q. Jin, J. Zhao, and G. Li. A microfluidic chip based on surfactant-doped polydimethylsiloxane (PDMS) in a sandwich configuration for low-cost and robust digital PCR. *Sensors and Actuators, B: Chemical*, 245:414–422, 2017. ISSN 09254005. doi: 10.1016/j.snb.2017.01.161.

R. Girones, M. A. Ferrús, J. L. Alonso, J. Rodriguez-Manzano, B. Calgua, A. de Abreu Corrêa, A. Hundesa, A. Carratala, and S. Bofill-Mas. Molecular detection of pathogens in water - The pros and cons of molecular techniques, 2010. ISSN 00431354.

R. Hall Sedlak and K. R. Jerome. The potential advantages of digital PCR for clinical virology diagnostics, 2014. ISSN 17448352.

A. C. Hatch, J. S. Fisher, S. L. Pentoney, D. L. Yang, and A. P. Lee. Tunable 3D droplet self-assembly for ultra-high-density digital micro-reactor arrays. *Lab on a Chip*, 11(15): 2509, 2011a. ISSN 1473-0197. doi: 10.1039/c0lc00553c. URL http://xlink.rsc.org/?DOI=c0lc00553c.

A. C. Hatch, J. S. Fisher, A. R. Tovar, A. T. Hsieh, R. Lin, S. L. Pentoney, D. L. Yang, and A. P. Lee. 1-Million droplet array with wide-field fluorescence imaging for digital PCR. *Lab on a Chip*, 11(22):3838, 2011b. ISSN 1473-0197. doi: 10.1039/c1lc20561g. URL http://xlink.rsc.org/?DOI=c1lc20561g.

K. A. Heyries, C. Tropini, M. Vaninsberghe, C. Doolin, O. I. Petriv, A. Singhal, K. Leung, C. B. Hughesman, and C. L. Hansen. Megapixel digital PCR. *Nature Methods*, 8(8): 649–651, 2011. ISSN 15487091. doi: 10.1038/nmeth.1640.

E. D. Hilborn, T. J. Wade, L. Hicks, J. Carpenter, B. Mull, J. Yoder, V. Roberts, and J. W. Gargano. Surveillance for waterborne disease outbreaks associated with drinking water and other nonrecreational water - United States, 2009-2010. *MMWR. Morbidity*

and mortality weekly report, 62(35):714–20, 2013. ISSN 1545-861X. URL http://www.ncbi.nlm.nih.gov/pubmed/24005226.

H. Kato, A. Yoshida, T. Ansai, H. Watari, T. Notomi, and T. Takehara. Loop-mediated isothermal amplification method for the rapid detection of Enterococcus faecalis in infected root canals. *Oral Microbiology and Immunology*, 22(2):131–135, 2007. ISSN 09020055. doi: 10.1111/j.1399-302X.2007.00328.x.

J. Lin and A. Ganesh. Water quality indicators: Bacteria, coliphages, enteric viruses, 2013. ISSN 09603123.

S. Y. Moorcraft, D. Gonzalez, and B. A. Walker. Understanding next generation sequencing in oncology: A guide for oncologists, 2015. ISSN 18790461.

T. Notomi, H. Okayama, H. Masubuchi, T. Yonekawa, K. Watanabe, N. Amino, and T. Hase. Loop-mediated isothermal amplification of DNA. *Nucleic Acids Research*, 28(12):E63, 2000. ISSN 1362-4962. doi: 10.1093/nar/28.12.e63. URL http://nar.oxfordjournals.org/content/28/12/e63.abstract{%}5Cnhttp://nar.oxfordjournals.org/content/28/12/e63.full.pdf{%}5Cnhttp://nar.oxfordjournals.org/content/28/12/e63.short{%}5Cnhttp://www.ncbi.nlm.nih.gov/pubmed/10871386.

V. C. Obuseng and F. Nareetsile. Bile Acids As Specific Faecal Pollution Indicators in Water and Sediments. *European Scientific Journal*, 9(12):273–286, 2013.

K. R. Pandit, P. E. Rueger, R. V. Calabrese, S. R. Raghavan, and I. M. White. Assessment of surfactants for efficient droplet PCR in mineral oil using the pendant drop technique. *Colloids and Surfaces B: Biointerfaces*, 126:489–495, 2015. ISSN 18734367. doi: 10.1016/j.colsurfb.2015.01.001.

B. H. Park, S. J. Oh, J. H. Jung, G. Choi, J. H. Seo, D. H. Kim, E. Y. Lee, and T. S. Seo. An integrated rotary microfluidic system with DNA extraction, loop-mediated isothermal amplification, and lateral flow strip based detection for point-of-care pathogen diagnostics. *Biosensors and Bioelectronics*, 91:334–340, 2017. ISSN 18734235. doi: 10.1016/j.bios.2016.11.063.

N. M. Quijada, G. Fongaro, C. R. Barardi, M. Hernández, and D. Rodríguez-Lázaro. Propidium monoazide integrated with qPCR enables the detection and enumeration of infectious enteric RNA and DNA viruses in clam and fermented sausages. *Frontiers in Microbiology*, 7(DEC), 2016. ISSN 1664302X. doi: 10.3389/fmicb.2016.02008.

F. Y. Ramírez-Castillo, A. Loera-Muro, M. Jacques, P. Garneau, F. J. Avelar-González, J. Harel, and A. L. Guerrero-Barrera. Waterborne pathogens: detection methods and challenges. *Pathogens (Basel, Switzerland)*, 4(2):307–34, 2015. ISSN 2076-0817. doi: 10.3390/pathogens4020307. URL http://www.pubmedcentral.nih.gov/articlerender.fcgi?artid=4493476{&}tool=pmcentrez{&}rendertype=abstract.

M. Rhee, Y. K. Light, R. J. Meagher, and A. K. Singh. Digital Droplet Multiple Displacement Amplification (ddMDA) for Whole Genome Sequencing of Limited DNA Samples. *PloS one*, 11(5):e0153699, 2016. ISSN 19326203. doi: 10.1371/journal.pone.0153699.

E. Rochelle-Newall, T. M. H. Nguyen, T. P. Q. Le, O. Sengtaheuanghoung, O. Ribolzi, O. Sengteheuanghoung, O. Ribolzi, O. Sengtaheuanghoung, and O. Ribolzi. A short review of fecal indicator bacteria in tropical aquatic ecosystems: knowledge gaps and future directions. *Frontiers in Microbiology*, 6(308):308, 2015. ISSN 1664302X. doi: http://dx.doi.org/10.3389/fmicb.2015.00308. URL http://journal.frontiersin.org/article/10.3389/fmicb.2015.00308/pdf{%}5Cnhttp://ovidsp.ovid.com/ovidweb.cgi?T=JS{&}CSC=Y{&}NEWS=N{&}PAGE=fulltext{&}D=emed18b{&}AN=603605973{%}5Cnhttp://ovidsp.ovid.com/ovidweb.cgi?T=JS{&}CSC=Y{&}NEWS=N{&}PAGE=fulltext{&}D=prem{&}AN=25941519.

O. Savichtcheva and S. Okabe. Alternative indicators of fecal pollution: Relations with pathogens and conventional indicators, current methodologies for direct pathogen monitoring and future application perspectives, 2006. ISSN 00431354.

F. Schuler, F. Schwemmer, M. Trotter, S. Wadle, R. Zengerle, F. von Stetten, and N. Paust. Centrifugal step emulsification applied for absolute quantification of nucleic acids by digital droplet RPA. *Lab Chip*, 15(13):2759–2766, 2015. ISSN 1473-0197. doi: 10.1039/C5LC00291E. URL http://xlink.rsc.org/?DOI=C5LC00291E.

F. Schuler, C. Siber, S. Hin, S. Wadle, N. Paust, R. Zengerle, and F. von Stetten. Digital droplet LAMP as a microfluidic app on standard laboratory devices. *Anal. Methods*, 8 (13):2750–2755, 2016. ISSN 1759-9660. doi: 10.1039/C6AY00600K. URL http://xlink.rsc.org/?DOI=C6AY00600K.

R. Shih and A. P. Lee. Post-Formation Shrinkage and Stabilization of Microfluidic Bubbles in Lipid Solution. *Langmuir*, 32(8):1939–1946, 2016. ISSN 15205827. doi: 10.1021/acs.langmuir.5b03948.

M. G. Simon and A. P. Lee. Microfluidic droplet manipulations and their applications. In *Microdroplet Technology: Principles and Emerging Applications in Biology and Chemistry*, pages 23–50. 2012. ISBN 9781461432654. doi: 10.1007/978-1-4614-3265-4_2.

L. W. Sinton, C. H. Hall, P. A. Lynch, and R. J. Davies-Colley. Sunlight inactivation of fecal indicator bacteria and bacteriophages from waste stabilization pond effluent in fresh and saline waters. *Applied and Environmental Microbiology*, 68(3):1122–1131, 2002. ISSN 00992240. doi: 10.1128/AEM.68.3.1122-1131.2002.

S. Sutton. The Most Probable Number Method and its uses in enumeration, qualification, and validation. *Journal of Validation Technology*, 16(3):35–38, 2010. ISSN 1079-6630. doi: 10.1097/RLI.0b013e318234e75b.Compartmental.

T. F. Tadros. Emulsion Formation,Stability, and Rheology. *Emulsion Formation and Stability*, pages 1–76, 2013. ISSN 3527647945. doi: 10.1002/9783527647941.ch1.

S. Tang and G. Whitesides. Basic microfluidic and soft lithographic techniques. In *Optofluidics: Fundamentals, Devices, and Applications*, pages 7–32. 2010. ISBN 0071601562. doi: 10.1002/1521-4095(200107)13:14⟨1053::AID-ADMA1053⟩3.0.CO;2-7. URL http://www2.egr.uh.edu/{~}nvaradar/private/Refs/Litho.pdf.

J. Teng, F. Yuan, Y. Ye, L. Zheng, L. Yao, F. Xue, W. Chen, and B. Li. Aptamer-based technologies in foodborne pathogen detection, 2016. ISSN 1664302X.

WHO/UNICEF. 2015 Update and MDG Assessment. *World Health Organization*, page 90, 2015. ISSN 0717-6163. doi: 10.1007/s13398-014-0173-7.2.

P. Woomer, J. Bennett, and R. Yost. Overcoming the Inflexibility of Most-Probable-Number Procedures. *Agronomy Journal*, 82(2):349, 1990. doi: 10.2134/agronj1990.00021962008200020035x.

K. Yang, J. LeJeune, D. Alsdorf, B. Lu, C. K. Shum, and S. Liang. Global distribution of outbreaks of water-associated infectious diseases. *PLoS Neglected Tropical Diseases*, 6(2), 2012. ISSN 19352727. doi: 10.1371/journal.pntd.0001483.

X. Zhao, J. Zhong, C. Wei, C.-W. Lin, and T. Ding. Current Perspectives on Viable but Non-culturable State in Foodborne Pathogens. *Frontiers in Microbiology*, 8:580, 2017. ISSN 1664-302X. doi: 10.3389/fmicb.2017.00580. URL http://www.ncbi.nlm.nih.gov/pubmed/28421064{%}5Cnhttp://www.pubmedcentral.nih.gov/articlerender.fcgi?artid=PMC5378802{%}5Cnhttp://journal.frontiersin.org/article/10.3389/fmicb.2017.00580/full.

Appendix A

Measurement of droplet size

A.1 Spatial calibration

Droplet size measurement was achieved using Image J. By Image J default settings, the droplet dimension would be measured in pixels. A spatial calibration was involved in droplet image processing to convert the pixel value to the real spatial unit, μm. As shown in Figure A.1, a pixel to micron conversion was determined by comparing the default measurement with the known dimensions.

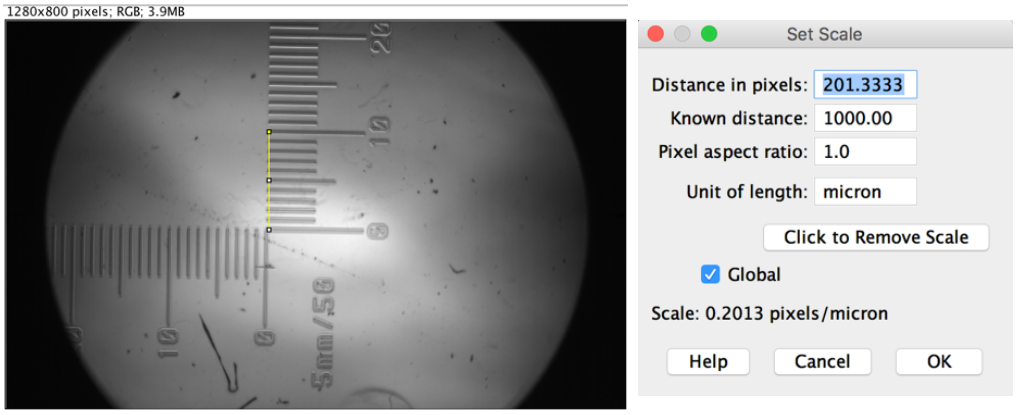

Figure A.1: Spatial calibration

A global scale was applied in the measurement of droplet images taken at the same magnification with the same microscope. After the spatial calibration, droplet diameter would be measured in micron.

A.2 Coefficient of variation (CV) of droplet diameter

Size uniformity of droplet is essential for droplet LAMP data quantification. The coefficient of variation of droplet diameter was determined using 400 sets of droplet measurement data obtained from 5 individual experiments (droplets were generated with the same LAMP sample and oil flow rates in all experiments). The average diameter of droplet was 55 μm with a CV value less then 4%.

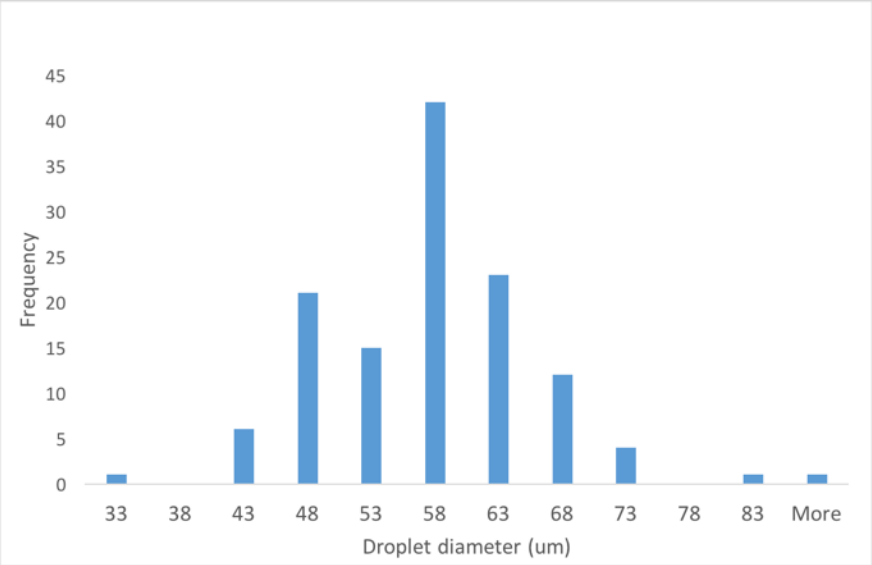

Figure A.2: Histogram of diameter of droplets.

Appendix B

Fluorescence image processing

Fluorescence image processing and quantitative droplet data acquisition were performed using Image J software. After each droplet LAMP test, five pairs of images were captured from the five different areas in droplet viewing chamber. The bright-field image was used for quantifying the total number of droplet in each area. With the fluorescent droplet counts from fluorescence images, the fraction of positive droplet could be obtained and then used for quantitative data computation.

The original color image was converted to gray-scale image, and a built in "threshold" function was used to convert the image to binary. "Watershed" and "Erode" algorithms were applied in the segmentation of overlapping droplets. The built in particle analyzer was used to measure the diameter and fluorescence intensity (gray value) of droplets and quantify the fluorescent droplets automatically. The upper and lower boundaries were set for droplet size and circularity. Droplet with a value outside the valid ranges would be excluded. Regions of interest (ROI) were created after the measurement of selected droplets, which could be used to calibrate droplet counts.

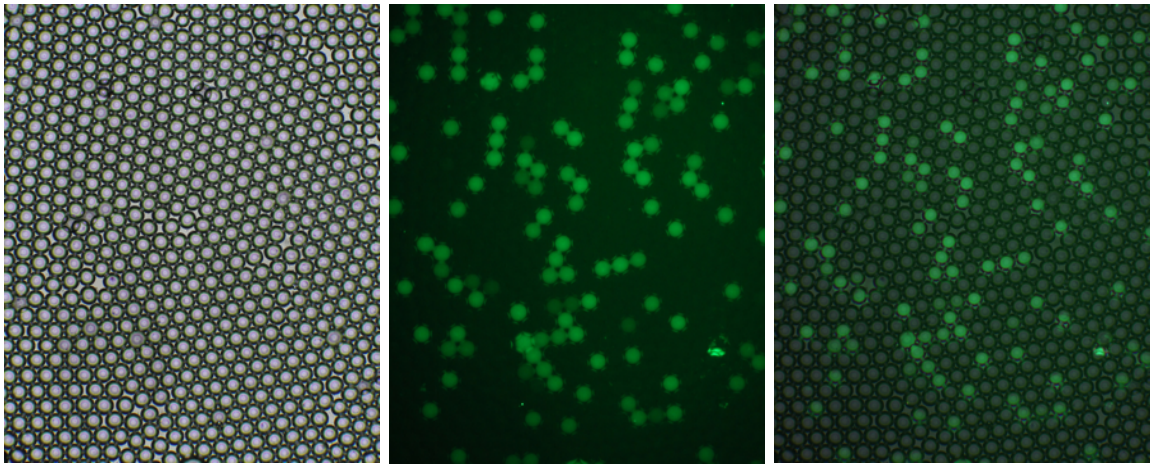

(a) (b) (c)

Figure B.1: Original droplet images. (a) Bright-field droplet image; (b) Fluorescence image captured from the same area. (c) composite image created using *Adobe*®*Photoshop*®.

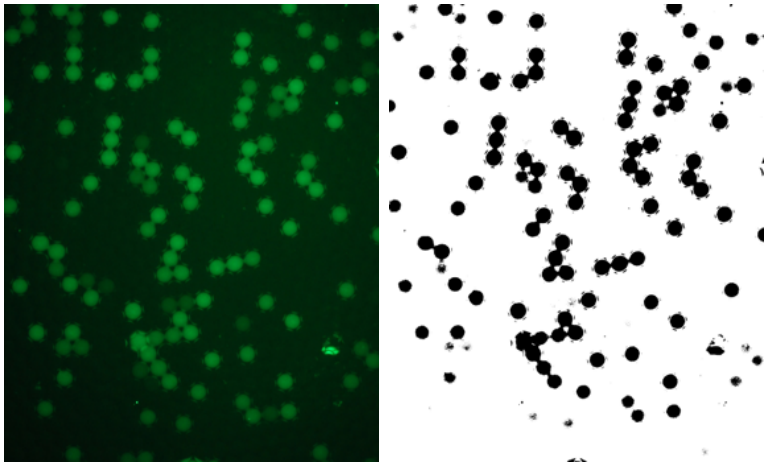

Figure B.2: (a) Original fluorescence image; (b) Binary image after image thresholding

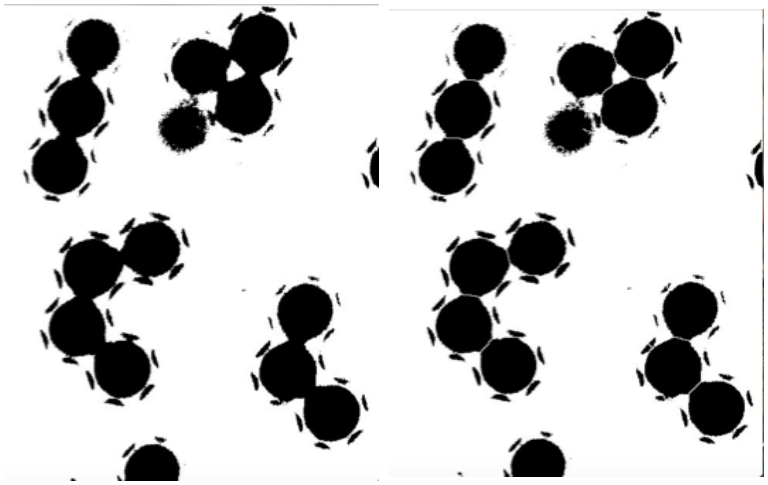

(a) overlapping droplets (b) separated droplets

Figure B.3: overlapping droplets segmentation using "watershed" and "erode" algorithms

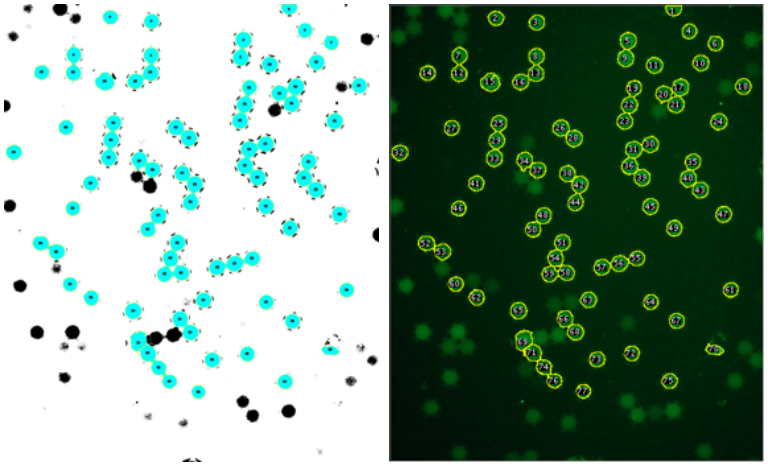

Figure B.4: (a) Automatic droplet quantification using particle analyzer; (b) Regions of interests defined by Image J

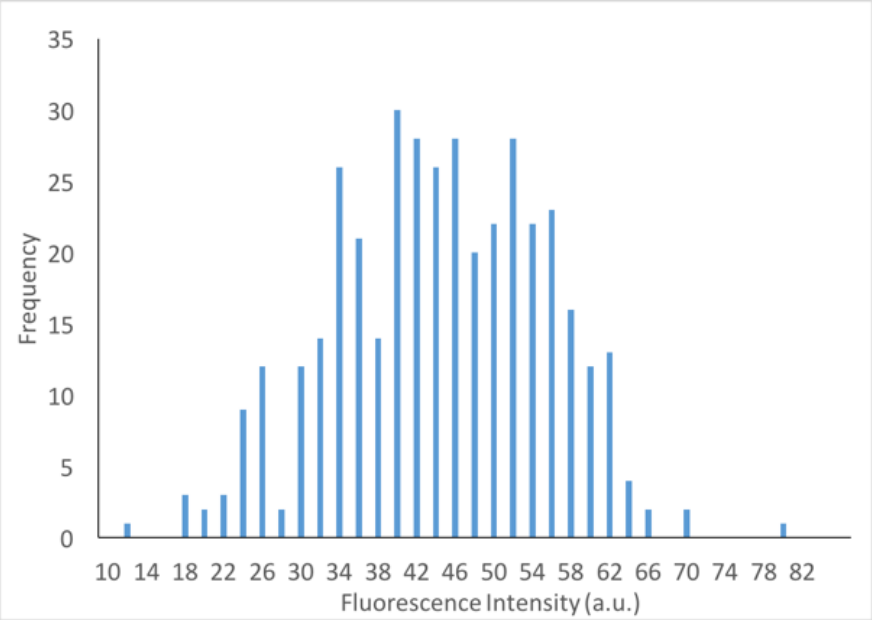

Figure B.5: Histogram of fluorescence intensity of droplets

Appendix C

Droplet quantification raw data

Expected Conc. (CFU/μl)	N_T	N_P	N_p/N_t	Conc. (CFU/μl)	Conc. (CFU/rxn)	Average (CFU/rxn)	S.D.
	730	0	0.0000	0	0		
	718	1	0.0014	15	31		
4.0E+00	748	1	0.0013	15	30	17812	4268.09
	634	0	0.0000	0	0		
	739	0	0.0000	0	0		
	778	3	0.0039	43	86		
	721	3	0.0042	46	93		
4.0E+01	783	6	0.0077	86	171	4182	247.40
	847	4	0.0047	53	105		
	769	6	0.0078	87	174		
	942	17	0.0180	202	405		
	971	15	0.0154	173	346		
4.0E+02	957	11	0.0115	129	257	331	53.76
	935	13	0.0139	156	311		
	938	14	0.0149	167	334		
	794	144	0.1814	2224	4449		
	812	142	0.1749	2137	4274		
4.0E+03	805	132	0.1640	1991	3982	126	43.28
	846	135	0.1596	1933	3865		
	925	164	0.1773	2169	4339		
	927	418	0.4509	6664	13329		
	922	408	0.4425	6495	12991		
4.0E+04	906	546	0.6026	10260	20519	12	16.64
	934	580	0.6210	10785	21570		
	952	576	0.6050	10327	20654		
4.0E+05	781	775	0.9923	54123	108246	0	0

Table C.1: raw data

Expected Conc. (CFU/μl)	N_T	N_P	N_p/N_t	Conc. (CFU/μl)	Conc. (CFU/rxn)	Average (CFU/rxn)	S.D.
	1019	3	0.0029	33	66		
	1001	3	0.0030	33	67		
5.2E+02	992	3	0.0030	34	67	62	9.95
	994	2	0.0020	22	45		
	981	3	0.0031	34	68		
	982	10	0.0102	114	228		
	1012	11	0.0109	121	243		
5.2E+03	1022	8	0.0078	87	175	183	53.79
	972	7	0.0072	80	161		
	1019	5	0.0049	55	109		
	867	65	0.0750	866	1733		
	946	74	0.0782	905	1811		
5.2E+04	972	72	0.0741	856	1711	1641	239.22
	895	67	0.0749	865	1730		
	769	41	0.0533	609	1218		

Table C.2: OCSD raw data

Expected Conc. (CFU/μl)	N_T	N_P	N_p/N_t	Conc. (CFU/μl)	Conc. (CFU/rxn)	Average (CFU/rxn)	S.D.
	-	0	0	0	0		
	-	0	0	0	0		
4.8E+02	-	0	0	0	0	0	-
	-	0	0	0	0		
	-	0	0	0	0		
	649	0	0	0	0		
	1005	0	0	0	0		
4.8E+03	857	0	0	0	0	21	31.04
	653	1	0.0015	17	34		
	640	2	0.0031	35	70		
	989	123	0.1244	1476	2953		
	1027	117	0.1139	1345	2689		
4.8E+04	1036	121	0.1168	1381	2761	2682	200.02
	1050	108	0.1029	1207	2413		
	1036	114	0.1100	1296	2592		

Table C.3: SD Creek raw data